ditional washes in PBS, 3,3'-diaminobenzidine tetrahydrochloride (DAB) was applied then sections were counterstained with hematoxylin. The entire procedure with the exception of incubation with primary antibody was conducted at room temperature. Formalin-fixed, paraffin-embedded sections of human uterine adenocarcinoma expressing RCAS1 protein were used as positive controls for RCAS1. Non-immunized mouse IgM for RCAS1 was substituted for the primary antibody in negative controls.

CD45 (leukocyte common antigen) staining. To identify infiltration by TILs, paraffin-embedded gastric adenocarcinoma sections were stained for CD45 (leukocyte common antigen). Deparaffinized and rehydrated sections were microwave irradiated in 10 m*M* sodium citrate (pH 6.0) for 10 min at 500 W. After cooling by immersion in PBS, sections were blocked with serum (Histofine SAB-AP kit; Nichirei, Tokyo) for 30 min and incubated with mouse anti-human CD45 monoclonal IgG (Dako, Carpinteria, CA) diluted at 1:70 for 60 min. All incubations proceeded at room temperature. After three washes in 0.1 *M* Tris-buffered saline (TBS), sections were incubated with biotinylated secondary antibody for 30 min. Sections were then washed three times in TBS and incubated with streptavidin-conjugated alkaline phosphatase for 30 min. After three additional washes in TBS, alkaline phosphatase substrate (fast blue) was applied. CD45-positive immunocytes appeared blue when viewed under a light microscope, and the morphology was almost exclusively lymphoid (i.e., TILs).

Immunocyte cell death detection by CD45/TUNEL dual staining. We detected apoptotic cells and bodies by terminal deoxynucleotidyl transferase-mediated deoxyuridine triphosphate nick end labeling (TUNEL) using an *in situ* Apoptosis Detection Kit (TaKaRa Biomedicals, Kyoto) according to the manufacturer's instructions. CD45/TUNEL dual staining allowed apoptotic TILs to be identified and quantified. Gastric adenocarcinoma sections were initially stained for CD45 as described. Following digestion with proteinase K (0.2 μg/ml in 10 m*M* Tris-Cl, pH 7.6) for 30 min, sections were washed in PBS and endogenous peroxidase activity was blocked with 3% hydrogen peroxide in methanol for 30 min. After three washes in PBS, sections were incubated with terminal deoxynucleotidyl transferase (TdT) in a humid chamber at 37°C for 60 min. TdT was omitted from negative control slides, which were included in each run. To localize cells containing labeled DNA strand breaks, sections were washed and incubated with sheep anti-fluorescein Ab Fab fragment conjugated with horseradish peroxidase in a humid chamber at 37°C for 30 min. After washing, TUNEL-positive color (red) was developed by incubating the sections with aminoethylcarbasol (AEC). When viewed under a light microscope, CD45-positive cells were stained blue, while CD45/TUNEL dual staining positive cells had a red nucleus and blue cytoplasm/surface.

Cell counting and labeling indices. One or two representative tissue sections were taken from each tumor, and the whole areas were surveyed under a microscope at ×100 magnification. Cells were counted at ×400 magnification in at least five random fields. The RCAS1 labeling index was defined as the percentage of tumor cells displaying immunoreactivity in the cytoplasm or on the membrane among 1000 tumor cells in each section. Tissue sections with less than 5% reactive cells were defined as negative, and those with more than 5% reactive cells were defined as positive, following previous reports.[5]

To quantify the infiltration of CD45-positive cells and apoptosis of these cells in RCAS1-positive and negative tumor regions of gastric cancer, sections were analyzed under light microscopy as follows. RCAS1-positive and RCAS1-negative tumor regions were located on a RCAS1-stained gastric tumor section by one investigator. A consecutive, CD45-stained slide from the same tumor was superimposed on the RCAS1-stained slide. Using histological landmarks, the corresponding RCAS1-positive and negative areas were located on the superimposed slide. The RCAS1-stained section was removed, and a second investigator, who was blinded to the local status of RCAS1, counted the number of CD45-positive cells in the area located by the first investigator. A similar approach was used to enumerate CD45/TUNEL dual-positive TILs within RCAS1-positive and negative areas of gastric cancer. Labeling indices of TIL infiltration are expressed as the percentage of CD45-positive cells per 2000 total nuclei counted at ×400 magnification. Labeling indices of TIL apoptosis are expressed as the percentage of CD45/TUNEL dual-positive cells per 500 total CD45-positive cells counted at ×400 magnification.

Statistical analysis. Differences between groups were analyzed using the χ^2 test, Fisher's exact test or Student's paired *t* test. Differences in the averages of labeling indices for TIL infiltration and apoptosis between RCAS1-positive and negative areas of gastric cancer were compared using the Wilcoxon signed-rank test for matched pairs. Values of $P<0.05$ were considered to indicate statistical significance, and all tests were two-sided.

Results

RCAS1 expression in gastric tissues. Immunohistochemical staining revealed RCAS1-positivity in 100% of normal gastric epithelial cells, 90% of intestinal metaplasia, 80% of gastric adenomas and 96% of gastric cancers (Table 1). We identified two expression patterns of RCAS1 in gastric cancer cells. Granular staining enriched in the glandular side of cytoplasm with polarity was defined as a P pattern, and granular staining scattered diffusely in the cytoplasm and on the cell membranes was defined as a D pattern (Fig. 1). The D pattern predominated in 33 of 54 gastric cancers (61%). Otherwise, the P pattern predominated in intestinal metaplastic mucosa and gastric adenomas. Normal gastric epithelial cells were homogeneously stained in the cytoplasm and on the cell membranes, and granular staining was not evident.

Relationship between RCAS1 expression and clinicopathological variables in gastric cancer. Clinicopathological variables did not significantly differ between RCAS1-positive and negative gas-

Table 1. RCAS1 expression in non-cancerous legions and cancer of the stomach

Pathological Diagnosis	No. of samples	No. of positive samples (%)			No. of negative samples (%)
		P[1]	D[2]	Others[3]	
Normal	5	0	0	5 (100)	0
Metaplasia	10	9 (90)	0	0	1 (10)
Adenoma	5	4 (80)	0	0	1 (20)
Cancer	54	19 (35)	33 (61)	0	2 (4)

1) P, P pattern; granular staining enriched in the glandular side of the cytoplasm with polarity.
2) D, D pattern; granular staining diffused throughout the cytoplasm and on the cell membranes.
3) Others, homogeneous staining in the cytoplasm without granular staining.

tric cancers. Table 2 shows the relationships between the two patterns of RCAS1 expression and the clinicopathological variables in gastric cancers. There was a significant relationship between the RCAS1 expression pattern and histological type ($P<0.005$). Nineteen of 39 intestinal type carcinomas (49%) showed the P pattern, and all of 13 diffuse type carcinomas (100%) showed the D pattern. Moreover, the D pattern of gastric cancers was more frequently recognized in carcinomas with large size ($P<0.01$), in those with invasion beyond the submucosa ($P<0.01$) and in those with regional lymph node metastasis ($P<0.05$), compared with the P pattern. Of the clinical variables, histological type was the most important factor according to the Cox proportional hazard analysis (data not shown). Neither gender nor age was associated with the RCAS1 staining pattern.

Table 2. Two patterns of RCAS1 staining in gastric cancer

Characteristics	RCAS1 staining pattern		*P* value
	P	D	
No. of cases	19	33	
Gender			
Male	15	23	n. s.[1]
Female	4	10	
Age	68.0±6.6	65.7±12.0	n. s.
Size (mm)	22.7±25.9	34.4±22.3	<0.01
Depth of invasion			
Mucasa	13	8	<0.01
Submucosa	4	13	
Muscularis propria	2	4	
Subserosa	0	5	
Penetrates serosa	0	3	
Histological type			
Intestinal	19	20	<0.005
Diffuse	0	13	
L/N metastasis			
Positive	2	14	<0.05
Negative	17	19	

1) n. s., not significant.

Decreased infiltration and increased apoptosis of TILs in RCAS1-expressing tumor regions. All gastric cancers contained infiltrates of cells that were immunohistochemically positive for CD45 and almost exclusively of lymphoid morphology, indicating that they were TILs. To evaluate whether RCAS1 expression on gastric cancers limited immune effector cell infiltration within tumors, we counted and compared the TILs in RCAS1-positive and negative tumor regions on the same sections (Table 3). Of all gastric cancers examined, only 10 contained separate RCAS1-positive and negative tumor regions in the same sections. The other samples had RCAS1-positive and negative tumor cells mixed together in the same tumor nests throughout the sections. Since RCAS1-positive and negative tumor regions were not separated, they could not be compared. In the 10 sections that were suitable for analysis, the amount of TIL infiltration was significantly reduced in RCAS1-expressing tumor regions (Fig. 2). The RCAS1 expression was associated with a statistically significant, twofold (mean) reduction in TILs in RCAS1-positive tumor regions when compared with RCAS1-negative tumor regions within the same sections ($P<0.01$). Thus, RCAS1 expression in gastric cancer appears to dramatically inhibit TIL infiltration of the tumor.

We investigated by CD45/TUNEL dual staining whether the diminished infiltration of TILs observed in RCAS1-expressing

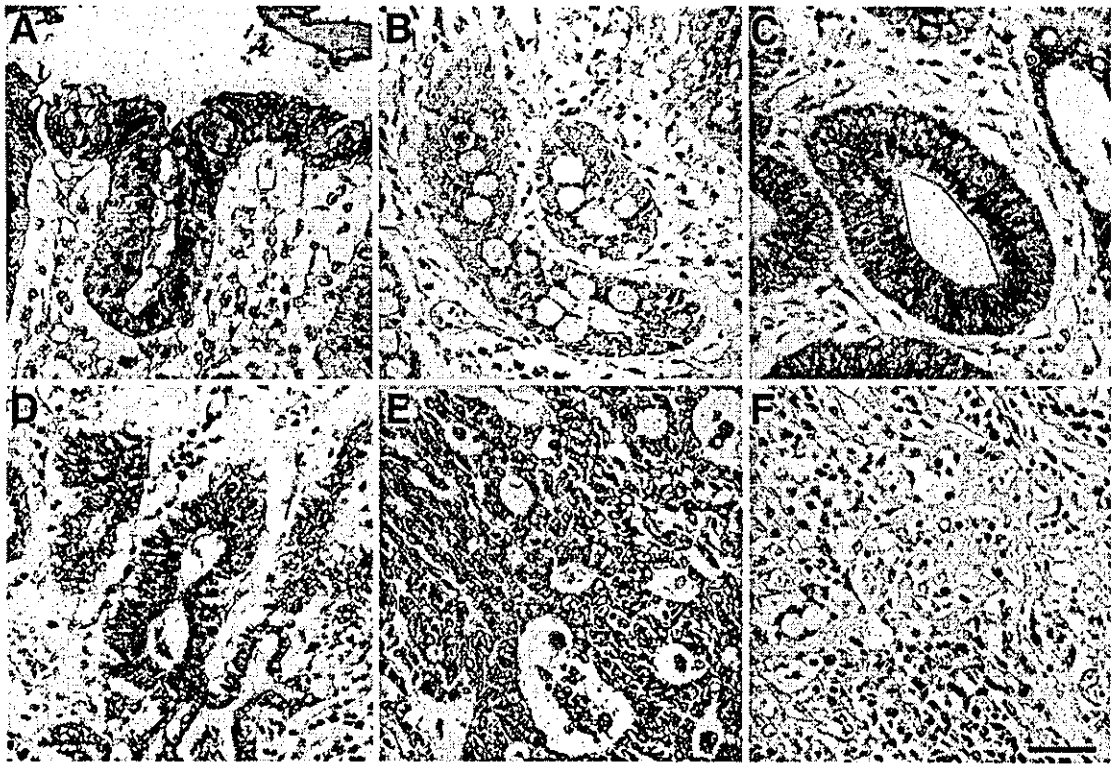

Fig. 1. Immunohistochemical stalning for RCAS1 expression in gastric tissues. Normal epithelial cells are homogeneously stained in cytoplasm and on cell membranes without granular staining (A). Intestinal metaplastic mucosa (B) and gastric adenoma (C) displayed only the P pattern (granular staining enriched in glandular side of cytoplasm with polarity). Expression patterns of RCAS1 in gastric cancer consist of the P pattern (D) and the D pattern (diffuse granular localization in cytoplasm and on cell membranes) (E). Rate of negative staining for RCAS1 is 4% (F). Scale bar, 100 μm.

Table 3. Labeling indices of TILs and rates of apoptosis of TILs in RCAS1-positive and negative regions on the same sections of gastric cancers

Tumor specimen	% RCAS1-positive cells	RCAS1-positive region		RCAS1-negative region	
		(% TILs)	(% apoptotic TILs)	(% TILs)	(% apoptotic TILs)
1	93	32.5	0.6	57.0	0.4
2	38	7.6	1.4	15.5	0.2
3	77	17.8	3.2	29.0	1.0
4	57	39.2	0.8	86.0	0.0
5	18	14.3	0.6	16.2	0.2
6	68	27.5	0.6	30.2	0.2
7	73	24.4	0.8	47.8	0.6
8	88	23.0	0.6	36.2	0.0
9	84	17.2	0.4	37.0	0.0
10	72	25.0	0.2	33.3	0.0
Mean	66.8	22.91[1)]	0.92[2)]	38.81[1)]	0.32[2)]

1) Mean % TILs was significantly lower in RCAS1-positive tumor regions than in RCAS1-negative tumor regions ($P<0.01$).
2) Mean % apoptotic TILs was significantly higher in RCAS1-positive tumor regions than in RCAS1-negative tumor regions ($P<0.01$).

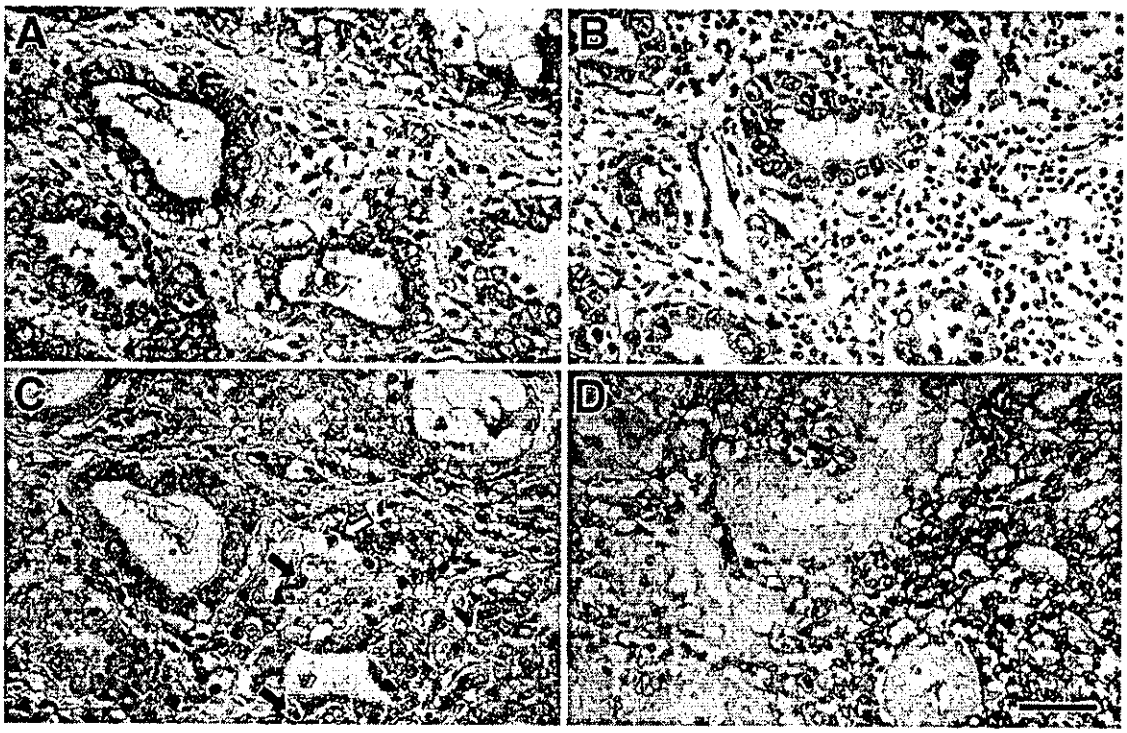

Fig. 2. Immunohistochemical staining identified RCAS1-positive (A) and negative (B) tumor regions on the same sections of gastric cancer. On consecutive tumor sections, apoptotic TILs were identified by CD45/TUNEL dual staining as blue CD45-positive cytoplasmic/cell surface with a brown TUNEL-positive nucleus (C and D). The white arrow shows an apoptotic tumor cell and black arrows are apoptotic TILs. Infiltration of TILs is reduced and apoptosis of TILs is increased in an RCAS1-positive area (C) and infiltration of TILs is increased and apoptosis of TILs is decreased in an RCAS1-negative area (D). Scale bar, 100 μm.

gastric cancer tissue was a result of apoptotic depletion (Fig. 2). The rates of apoptosis of TILs were quantified in RCAS1-positive and negative tumor regions of the same sections (Table 3). A statistically significant, threefold (mean) increase in the TUNEL-positive cell death of CD45-positive TILs was observed in RCAS1-positive tumor regions compared with RCAS1-negative tumor regions ($P<0.01$). The threefold increase in apoptosis of TILs associated with RCAS1-expressing tumor regions suggested that the apoptosis of TILs triggered by RCAS1 expressed by tumors contributed to the depletion of CD45-positive TILs in these areas.

Discussion

We demonstrated that the expression of RCAS1 was frequent in precancerous and cancerous gastric tissues. Immunohistochemically, RCAS1 was expressed in 96% (52/54 specimens) of gastric cancers. The incidence of RCAS1 expression in gastric cancers was similar to the reported levels,[12)] that are the highest among the various types of cancers investigated. Clinicopathological variables did not significantly differ between RCAS1-positive and negative gastric cancers. However, we discriminated two staining patterns of RCAS1 in gastric cancer cells: 1)

a localized, granular staining in the glandular side of cytoplasm with polarity (P pattern) and 2) diffuse granular staining in the cytoplasm and on the cell membrane (D pattern). The staining patterns correlated with size of tumors, depth of tumor invasion, histological type and lymph node metastasis. Among these clinical variables, histological type was the most important according to the Cox proportional hazards analysis (data not shown). In fact, 19 of 39 intestinal-type carcinomas (49%) had the P pattern, and all of 13 diffuse-type carcinomas (100%) had the D pattern. RCAS1 may be associated with differences in biological or pathogenetic characteristics between intestinal and diffuse types of gastric cancer. Moreover, the D pattern appeared to be associated with malignant nature of the cancer cells. The differences in the RCAS1 distribution might be related to differences of function, including a death ligand for immune cells, malignant transformation or progression. The two staining patterns of RCAS1 are barely discernible in other types of cancer.[5] One study of lung cancer indicates that RCAS1 is expressed intensely on the cell membrane of squamous cell carcinoma and diffusely in the cytoplasm of adenocarcinoma cells.[7] RCAS1 expression might reflect the biological features of each type of cancer. Further studies are required to determine differences in RCAS1 expression patterns.

RCAS1 was homogeneously expressed in normal gastric epithelial cells and the staining pattern did not correspond with either of the P or D patterns. RCAS1 is also expressed in normal uterine endometrial glands and normal bronchial ciliated columnar epithelial cells.[5,7] The biological functions of RCAS1 secreted by non-cancerous tissues remain to be investigated. Moreover, RCAS1 was expressed as the P pattern in all precancerous gastric tissues. RCAS1 might be a useful marker of malignant transformation and progression in gastric cancer.

RCAS1 expressed on tumor cells has been considered a death ligand that allows tumor cells to evade host immune surveillance.[6] In the present study, we first directly analyzed the effects of RCAS1 expression on TIL infiltration using tumor tissue specimens of gastric cancer, and demonstrated that RCAS1 expression was significantly associated with reduced infiltration of TILs and increased apoptosis of TILs. Previously, it was reported that apoptotic lymphocytes surround RCAS1-positive, but not RCAS1-negative Hodgkin and Reed-Sternberg cells of Epstein-Barr virus-associated Hodgkin's disease.[10] Thus, RCAS1 expressed on tumor cells unquestionably contributes to tumor escape from host immune surveillance by inducing the apoptosis of TILs. However, which populations of TILs (T cells, B cells, NK cells, dendritic cells or macrophages) are affected by the RCAS1 signal is not known. Even in RCAS1-positive tumor regions, significant numbers of TILs remained. This might be due to differences in the expression of RCAS1 receptor on these cells or in the sensitivity of RCAS1 to the signal.

The notion that RCAS1 expression on tumor cells induces apoptosis in RCAS1 receptor-positive immune cells is reminiscent of the case of Fas ligand (FasL)/Fas. Several investigators have demonstrated that FasL expressed on tumors engages the Fas receptor expressed on the surface of immune cells, causing them to undergo apoptosis and granting the tumor immune-privileged status.[15–17] Bennett *et al.* reported that FasL expression in esophageal and gastric cancers induced apoptosis of TILs.[18,19] We also examined the relationship between FasL expression and the number of TILs or apoptosis of TILs. However, in our series of 54 gastric cancers, FasL-positive areas were not separated from FasL-negative areas on the same section (data not shown).

Tumor cells acquire the ability to evade host immune surveillance through several strategies that include the secretion of immunosuppressive factors such as transforming growth factor-β and IL-10,[20,21] down-regulation of cell surface MHC class I expression[22,23] and expression of death ligands such as FasL on tumor cells.[24–26] Our results show that RCAS1 expressed on tumor cells is one mechanism through which tumors can escape host immune surveillance.

In conclusion, we observed two distinctive patterns of RCAS1 expression. We also demonstrated that RCAS1 might be a useful marker of malignant transformation and progression of gastric cancer, might reflect the biological characteristics of intestinal and diffuse types of gastric cancer, and might contribute to tumor escape from host immune surveillance by inducing the apoptosis of its receptor-positive TILs. Protecting TILs from RCAS1 could be a promising therapeutic strategy.

1. Karpeh MS, Kelsen DP, Tepper JE. Cancer of the stomach. In: Devita VT, Hellman S, Rosenberg SA, editors. Cancer: principles and practice of oncology. 6th ed. Philadelphia: Lippincott-Raven Publishers; 2001. p. 1092–126.
2. Itoh T, Ueda Y, Kawashima I, Nukaya I, Fujiwara H, Fuji N, Yamashita T, Yoshimura T, Okugawa K, Iwasaki T, Ideno M, Takesako K, Mitsuhashi M, Orita K, Yamagishi H. Immunotherapy of solid cancer using dendritic cells pulsed with the HLA-A24-restricted peptide of carcinoembryonic antigen. *Cancer Immunol Immunother* 2002; **51**: 99–106.
3. Inoue H, Mori M, Honda M, Li J, Shibuta K, Mimori K, Ueo H, Akiyoshi T. The expression of tumor-rejection antigen "MAGE" genes in human gastric carcinoma. *Gastroenterology* 1995; **109**: 1522–5.
4. Sonoda K, Nakashima M, Saito T, Amada S, Kamura T, Nakano H, Watanabe T. Establishment of a new human uterine cervical adenocarcinoma cell line, SiSo, and its reactivity to anti-cancer reagents. *Int J Oncol* 1995; **6**: 1099–104.
5. Sonoda K, Nakashima M, Kaku T, Kamura T, Nakano H, Watanabe T. A novel tumor-associated antigen expressed in human uterine and ovarian carcinomas. *Cancer* 1996; **77**: 1501–9.
6. Nakashima M, Sonoda K, Watanabe T. Inhibition of cell growth and induction of apoptotic cell death by the human tumor-associated antigen RCAS1. *Nat Med* 1999; **5**: 938–42.
7. Iwasaki T, Nakashima M, Watanabe T, Yamamoto S, Inoue Y, Yamanaka H, Matsumura A, Iuchi K, Mori T, Okada M. Expression and prognostic significance in lung cancer of human tumor-associated antigen RCAS1. *Int J Cancer* 2000; **89**: 488–93.
8. Takahashi H, Iizuka H, Nakashima M, Wada T, Asano K, Ishida-Yamamoto K, Watanabe T. RCAS1 antigen is highly expressed in extramammary Paget's disease and in advanced stage squamous cell carcinoma of the skin. *J Dermatol Sci* 2001; **2**: 140–4.
9. Oshima K, Muta K, Nakashima M, Haraoka S, Tutiya T, Suzumiya J, Kawasaki C, Watanabe T, Kikuchi M. Expression of human tumor-associated antigen RCAS1 in Reed-Sternberg cells in association with Epstein-Barr virus infection: a potential mechanism of immune evasion. *Int J Cancer* 2001; **93**: 91–6.
10. Noguchi K, Enjoji M, Nakamuta M, Nakashima M, Nishi H, Choi I, Taguchi K, Katoh K, Shimada M, Sugimachi K, Tsuneyoshi M, Nawata H, Watanabe T. Expression of a tumor-associated antigen RCAS1 in hepatocellular carcinoma. *Cancer Lett* 2001; **68**: 197–202.
11. Oizumi S, Yamazaki K, Nakashima M, Watanabe T, Hommura F, Ogura S, Nishimura M, Dosaka-Akita H. RCAS1 expression: a potential prognostic marker for adenocarcinomas of the lung. *Oncology* 2002; **62**: 333–9.
12. Kubokawa M, Nakashima M, Yao T, Ito K, Harada N, Nawata H, Watanabe T. Aberrant intracellular localization of RCAS1 is associated with tumor progression of gastric cancer. *Int J Oncol* 2001; **19**: 695–700.
13. Oshikiri T, Hida Y, Miyamoto M, Hashida H, Katoh K, Suzuoki M, Nakakubo Y, Hiraoka K, Shinohara T, Itoh T, Kondo S, Katoh H. RCAS1 as a tumour progression marker: an independent negative prognosis factor in gallbladder cancer. *Br J Cancer* 2001; **85**: 1922–7.
14. Laurèn P. The two histological main types of gastric carcinoma diffuse and so-called intestinal type carcinoma, an attempt at histoclinical classification. *Acta Pathol Microbiol Scand* 1965; **64**: 31–49.
15. Griffith TS, Brunner T, Fletcher SM, Green DR, Ferguson TA. Fas ligand-induced apoptosis as a mechanism of immune privilege. *Science* 1995; **270**: 1189–92.
16. Hahne M, Rimoldi D, Schroter M, Romero P, Schreier M, French LE, Schneider P, Bornand T, Fontana A, Lienard D, Certtini J-C, Tshhopp J. Melanoma cell expression of Fas (Apo-1/CD95) ligand: implications for tumor immune escape. *Science* 1996; **274**: 1363–6.

17. Strand S, Hofmann WJ, Hug H, Muller M, Otto G, Strand D, Mariani SM, Stremmel W, Krammer PH, Galle PR. Lymphocyte apoptosis induced by CD95 (APO-1/Fas) ligand-expressing tumor cells, a mechanism of immune evasion? *Nat Med* 1996; **2**: 1361–6.
18. Bennett MW, O'Connell J, O'Sullivan GC, Brady C, Roche D, Collins JK, Shanahan F. The Fas counterattack *in vivo*: apoptotic depletion of tumor-infiltrating lymphocytes associated with Fas ligand expression by human esophageal carcinoma. *J Immunol* 1988; **160**: 5669–75.
19. Bennett MW, O'Connell J, O'Sullivan GC, Roche D, Brady C, Kelly J, Collins JK, Shanahan F. Expression of Fas ligand by human gastric adenocarcinomas: a potential mechanism of immune escape in stomach cancer. *Gut* 1999; **44**: 156–62.
20. Samuels V, Barrett JM, Bockman S, Pantazis CG, Allen MB Jr. Immunocytochemical study of transforming growth factor expression in benign and malignant glioma. *Am J Pathol* 1989; **134**: 894–902.
21. Huettner C, Paulus W, Roggendorf W. Messenger RNA expression of the immunosuppressive cytokine IL-10 in human gliomas. *Am J Pathol* 1995; **146**: 317–22.
22. Imboden M, Murphy KR, Rakhmilevich AL, Neal ZC, Xiang R, Reisfeld RA, Gillies SD, Sondel PM. The level of MHC class I expression on murine adenocarcinoma can change the antitumor effector mechanism of immunocytokine therapy. *Cancer Res* 2001; **61**: 1500–17.
23. Goodenow RS, Vogel JM, Linsk RL. Histocompatibility antigens on murine tumors. *Science* 1985; **230**: 777–83.
24. Pitti RM, Marsters SA, Ruppert S, Donahue CJ, Moore A, Ashkenazi A. Induction of apoptosis by Apo-2 ligand, a new member of the tumor necrosis factor cytokine family. *J Biol Chem* 1996; **271**: 12687–90.
25. Wiley SR, Schooley K, Smolak PJ, Din WS, Huang C-P, Nicholl JK, Sutherland GR, Smith TD, Rauch C, Smith CA, Goodwin RG. Identification and characterization of a new member of the TNF family that induces apoptosis. *Immunity* 1995; **3**: 673–82.
26. Chicheportiche Y, Bourdon PR, Xu H, Hsu Y-M, Scott H, Hession C, Garcia I, Browning JL. TWEAK, a new secreted ligand in the tumor necrosis factor family that weakly induces apoptosis. *J Biol Chem* 1997; **272**: 32401–10.

CT-Guided Transbronchial Biopsy Using an Ultrathin Bronchoscope With Virtual Bronchoscopic Navigation*

Naofumi Shinagawa, MD; Koichi Yamazaki, MD, PhD; Yuya Onodera, MD; Kazuo Miyasaka, MD, PhD; Eiki Kikuchi, MD; Hirotoshi Dosaka-Akita, MD, PhD; and Masaharu Nishimura, MD, PhD

Study objectives: **We evaluated the feasibility, safety, and efficacy of CT-guided transbronchial biopsy (TBB) using an ultrathin bronchoscope with navigation by virtual bronchoscopy (VB) for small peripheral pulmonary lesions of < 20 mm in diameter.**

Design: **A pilot study.**

Setting: **A national university hospital.**

Patients: **We performed CT-guided TBB after VB navigation for 25 patients with 26 small peripheral pulmonary lesions (average diameter, 13.2 mm) between June 1, 2001, and October 31, 2002. Of the 26 lesions, 10 were in the right upper lobe, 2 were in the right middle lobe, 6 were in the right lower lobe, and 8 were in the left upper lobe. Nineteen lesions were not detected on chest radiographs.**

Interventions: **VB images were reconstructed from helical CT scans. CT-guided TBB was performed using an ultrathin bronchoscope after studying the VB image.**

Results: **CT-guided TBB was performed safely without any complications for all patients. The bronchi seen under VB imaging were highly consistent with the actual bronchi confirmed using an ultrathin bronchoscope. The ultrathin bronchoscope was inserted between the fifth and eighth generation bronchi. The average durations of the initial scan, the first biopsy, and the total examination were 5.46, 12.96, and 29.27 min, respectively. Seventeen lesions (65.4%) were diagnosed from pathology examinations (primary lung cancers, 13; atypical adenomatous hyperplasia, 1; metastatic cancer, 1; sarcoidosis, 1; and nontuberculous mycobacteriosis, 1). Diagnoses were not obtained for the remaining lesions due to an insufficient number of specimens (six specimens) or to the inability to reach the lesions even using the ultrathin bronchoscope (three specimens).**

Conclusions: **In summary, CT-guided TBB using an ultrathin bronchoscope with VB navigation was safely performed and was effective for diagnosing small peripheral pulmonary lesions.**

(CHEST 2004; 125:1138–1143)

Key words: benign disease; CT-guided transbronchial biopsy; primary lung cancer; small peripheral pulmonary lesion; stereotactic radiotherapy; ultrathin bronchoscope; virtual bronchoscopic navigation

Abbreviations: AAH = atypical adenomatous hyperplasia; FFB = flexible fiberoptic bronchoscope; HRCT = high-resolution CT; SRT = stereotactic radiotherapy; TBB = transbronchial biopsy; VB = virtual bronchoscopy

With recent advances in CT scan screening, an increase in the detection of faint nodules in the peripheral lung has been noted. The transbronchial approach using a flexible fiberoptic bronchoscope (FFB) remains one of the most feasible and safest methods of diagnosing those lesions. The accuracy of diagnosing peripheral pulmonary lesions from tissue samples retrieved using the FFB is reportedly 20 to 84% in cases of malignant lesions, and 35 to 56% in cases of benign lesions.[1–9] The yield of FFB is lower in peripheral lesions,[1,2,4–7] compared with those of central and intermediate lesions, and is lower in small lesions.[1–3,6–9] Baaklini and colleagues[1] reported that lesions < 2.0 cm in diameter had a diagnostic yield of 14% when located in the peripheral third, compared with 31% when located in the inner two thirds of the lung.

*From the First Department of Medicine (Drs. Shinagawa, Yamazaki, Kikuchi, and Nishimura), Department of Radiology (Drs. Onodera and Miyasaka), School of Medicine, and the Department of Medical Oncology (Dr. Dosaka-Akita), Graduate School of Medicine, Hokkaido University, Sapporo, Japan.

Manuscript received March 10, 2003; revision accepted August 11, 2003.

Correspondence to: Koichi Yamazaki, MD, PhD, First Department of Medicine, Hokkaido University School of Medicine, North 15, West 7, Kitaku, Sapporo 060-8638, Japan; e-mail: kyamazak@med.hokudai.ac.jp

Some respiratory physicians prefer to diagnose small peripheral pulmonary lesions from tissue samples obtained by percutaneous needle aspiration cytology or biopsy.[10–13] Although the success rates of these techniques might be very high, with 76 to 97% diagnostic accuracy,[14] these techniques have several problems. First, they have the potential to spread malignant cells from the tumor into the pleural cavity.[10,11] For patients with poor pulmonary function, these techniques result in an increased risk of pneumothorax. Moreover, systemic arterial air embolism is a rare but severe complication.[12,13] Conversely, video-assisted thoracoscopic biopsy may be appropriate for lesions that are strongly suspected to be malignant. However, this process is invasive for elderly patients and patients with poor respiratory function. Thus, diagnosing small peripheral pulmonary lesions more effectively using the FFB is important to respiratory physicians.

The following three methodological problems hinder the diagnosis of small peripheral pulmonary lesions using an FFB: (1) small peripheral pulmonary lesions may not be visible under fluoroscopic radiograph guidance; (2) curettage for transbronchial cytology can reach small peripheral pulmonary lesions, but not forceps for transbronchial biopsy (TBB), given the difficulty in maneuvering within the angles of the bronchi; and (3) identifying accessible bronchial routes to reach small peripheral pulmonary lesions is not always easy during limited examination time. CT-guided TBB or cytology has been developed to overcome the first problem of incorrect positioning of the forceps or curette.[15,16] To overcome the second problem, an ultrathin bronchoscope has been developed that can be inserted into more peripheral bronchi than conventional bronchoscopes under direct vision.[17,18] Recently, the working channel of an ultrathin bronchoscope has become wider, so the collection of tissue specimens has become possible. This has led to the feasibility of TBB for diagnosing more peripheral small lesions of the lung.[19,20] In addition, rapid progress in computer technology has resulted in advances in diagnostic imaging. Virtual bronchoscopy (VB) is the application of three-dimensional display techniques to the airways, enabling the simulation of actual bronchoscopic procedures. A new method using VB for navigation to the proper bronchi has been introduced to bronchoscopy.[21,22]

In the present study, CT-guided TBB, use of an ultrathin bronchoscope, and VB navigation were combined in one procedure. The feasibility, safety, and efficacy of this procedure for diagnosing small peripheral pulmonary lesions were evaluated.

Materials and Methods

Subjects

Between June 1, 2001, and October 31, 2002, at Hokkaido University Medical Hospital, 29 patients with 30 small peripheral pulmonary lesions (mean diameter, < 20 mm) underwent chest CT scans to generate VB images for the navigation of CT-guided TBB with an ultrathin bronchoscope. Nineteen lesions were not detected on chest radiographs, but by chest CT scans performed during the follow-up of other diseases or for check-ups of the lung. No patients with small peripheral pulmonary lesions < 20 mm in diameter received TBB without information about VB during this period, but lesions deemed as displaying inflammation or postinflammatory changes on high-resolution CT (HRCT) scans were excluded. For small peripheral pulmonary lesions of < 10 mm in diameter, only those proven to be growing were included in this study. All patients were given detailed descriptions of the examination and were informed that this was a new approach. Informed consent was obtained in all cases. Conventional and HRCT scan examinations were performed on all 29 patients before VB images were made.

VB

CT scan examinations were performed using a multidetector CT scanner (Aquilion; Toshiba; Tokyo, Japan) with the following parameters: collimation, 0.5 mm; four detectors; pitch, 5 to 7; and rotation time, 0.5 s. Helical volume data sets were acquired during single breath-hold inhalations. Images were reconstructed from helical CT scans and transferred to a computer workstation (Alatoview; Toshiba; or Virtual Place worksite; Medical Imaging Laboratory; Tokyo, Japan). All VB images were made by one radiologist. The volume-rendering method was used for the VB algorithm. VB objects were built by autosegmentation, and a fly-through image was used. Reconstructed VB images were generated accurately to approximately the fifth generation of bronchi, as more peripheral bronchi were not visible. We therefore generated VB images using the pulmonary artery instead of invisible peripheral bronchi to predict a more peripheral route (Y. Onodera, MD; unpublished observation; May 2003).

CT-Guided TBB

Each patient was premedicated using 15 mg pentazocine hydrochloride and 0.5 mg atropine sulfates. Local anesthesia of the upper respiratory tract was achieved using 4% lidocaine. All patients were intubated orally with an 8.0-mm endotracheal tube, as a routine procedure for TBB in our institute. In this study, an ultrathin bronchoscope (BF-type XP-40; Olympus; Tokyo, Japan) with an external diameter of 2.8 mm and a biopsy channel diameter of 1.2 mm was utilized. After the VB image was generated and studied, the ultrathin bronchoscope was inserted into the target bronchus as deep as possible under direct vision. The position of the forceps inserted through a bronchoscope then was confirmed and adjusted by real-time multislice CT scan. After the position was confirmed, a biopsy was performed. The bronchoscopy procedures were performed by two pulmonary fellows, each with > 5 years of training and experience in bronchoscopy, who were directly supervised and assisted by the pulmonary faculty in attendance.

Results

Twenty-nine patients with 30 small peripheral pulmonary lesions were enrolled into this study. One

patient was excluded because the lesion was no longer visible when the CT scan for VB was performed. VB images were therefore obtained from 28 patients with 29 small peripheral pulmonary lesions. Three patients with three lesions did not undergo CT-guided TBB, as the VB images suggested that the lesions would not be able to be reached using even an ultrathin bronchoscope. No bronchi reaching the lesions were seen.

Thus, a total of 25 patients (9 men, 16 women) with 26 small peripheral pulmonary lesions received CT-guided TBB. The average age was 67.1 years (age range, 57 to 82 years). On HRCT scans, the average diameter of target lesions was 13.2 mm. Of the 26 lesions, 10 were in the right upper lobe, 2 were in the right middle lobe, 6 were in the right lower lobe, and 8 were in the left upper lobe.

CT-guided TBB was performed safely without any complications for all 25 patients with 26 small peripheral pulmonary lesions. The bronchi depicted on VB images were highly consistent with the actual bronchi, as confirmed by ultrathin bronchoscopy (Fig 1). The ultrathin bronchoscope was inserted between the fifth and eighth generation bronchi. The tip of the ultrathin bronchoscope and the tip of the forceps were visualized clearly along with each lesion on real-time multislice CT scans in all cases, confirming the lesions as the origins of the specimens. The average time for an initial scan, including anesthesia of the trachea and bronchi, using an ultrathin bronchoscope and inserting the ultrathin bronchoscope following VB, was 5.46 min. The average time for the first biopsy, including the first scan, the CT scan, and the adjustment of positions for the bronchoscope and forceps, was 12.96 min. The average total time for examination once the ultrathin bronchoscope was inserted into the endotracheal tube was 29.27 min (Table 1). Light bleeding occurred around small peripheral pulmonary lesions, but severe bleeding was not observed under CT fluoroscopy.

Adequate tissue was obtained for pathologic diagnoses in 17 of the 26 lesions (65%) [Table 2]. Lesions comprised 13 cases of primary lung cancer (adeno-

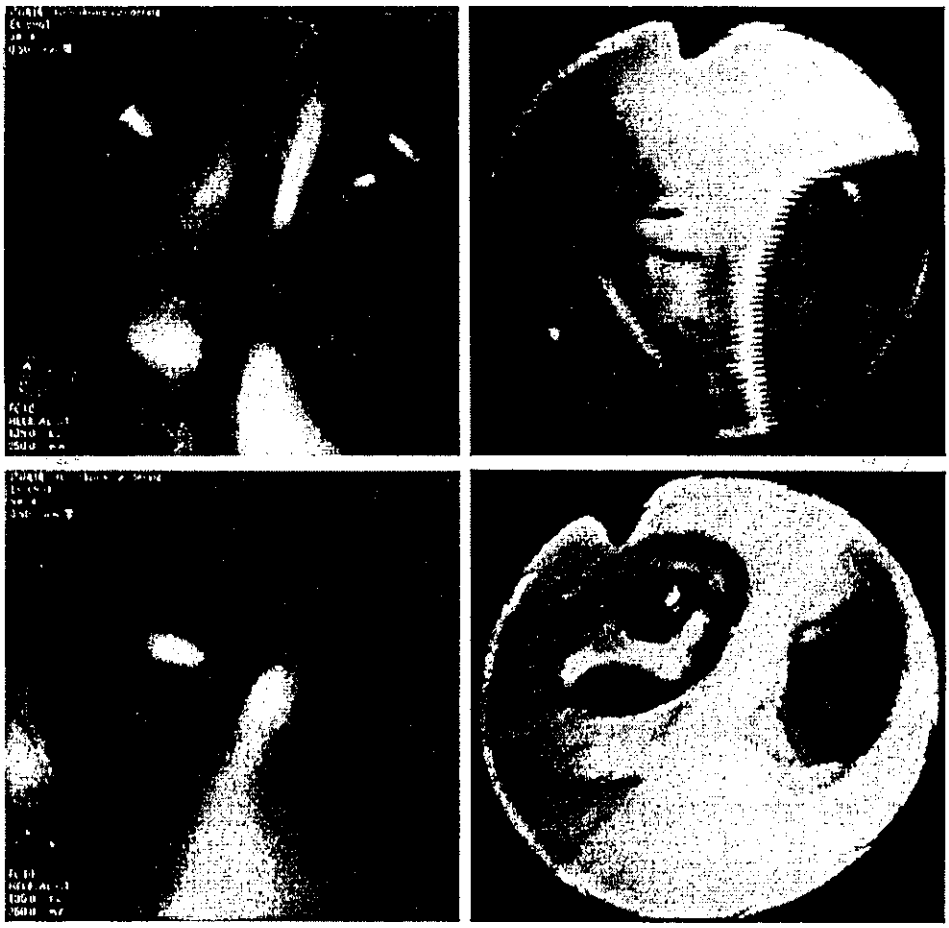

FIGURE 1. An example of bronchi seen on VB images (*left*), and images of actual bronchi seen using ultrathin bronchoscopy (*right*).

Table 1—*Duration of CT-Guided TBB*

Variables	Mean ± SD, min	Range, min
Time to first scan*	5.46 ± 2.25	0.85–10.45
Time to first biopsy†	12.96 ± 8.57	3.33–30.58
Total time‡	29.27 ± 13.09	9.90–55.45

*Including time to anesthetize bronchi using bronchoscope and insert bronchoscope following VB imaging.
†Including time for CT scan and adjusting position of bronchoscope and forceps.
‡Including time for inserting ultrathin bronchoscope into endotracheal tube.

carcinoma, 12 cases; large cell carcinoma, 1 case), 1 case of atypical adenomatous hyperplasia (AAH), 1 case of metastatic cancer of the colon, and 2 cases of benign disease (sarcoidosis, 1 case; nontuberculous mycobacteriosis, 1 case). Of these 17 lesions, 10 were treated by surgical resection. Five lesions diagnosed as primary lung cancer were treated with stereotactic radiotherapy (SRT), as a physical examination had revealed poor pulmonary or cardiac function. Two lesions diagnosed as benign lesions were monitored without intervening therapy. Of the nine lesions that could not be diagnosed by CT-guided TBB, five were treated by surgical resection. Four then were diagnosed as representing primary lung cancer, and one was diagnosed as AAH. The diagnostic sensitivity of this procedure was 65.4% for the 26 lesions in which CT-guided TBB was performed. Of the 22 lesions in which a final diagnosis was made, the sensitivity, specificity, negative predictive value, positive predictive value, and accuracy were 75.0%, 100.0%, 28.6%, 100.0%, and 77.3%, respectively.

No significant differences were observed regarding age, sex, average diameter or size of the lesion, time of the initial scan, time of the first biopsy, total time of the examination, the number of biopsies, or the ability to obtain a diagnosis (data not shown). Of the nine lesions for which diagnoses could not be obtained, six lesions had an insufficient number of biopsy samples taken and the other three lesions were inaccessible, even using an ultrathin bronchoscope with VB navigation.

Table 2—*Diagnosis and Treatment of Examined Lesions*

CT-Guided TBB Procedure	Lesions, No.	Treatment	Lesions, No.
Diagnosed			
Lung cancer		Surgery	11
Adenocarcinoma	12	Radiotherapy	4
Large cell carcinoma	1	Observation	2
Metastasis of colon cancer	1		
Nontuberculous Mycobacterium	1		
Sarcoidosis	1		
AAH	1		
Total	17 (65%)		17 (65%)
Not diagnosed			
Treatment			
Surgery*	5		
Observation	4		
Total	9 (35%)		

*Lung cancer, 4; AAH, 1.

Discussion

A transbronchial approach under radiograph fluoroscopic guidance has been the most generally accepted method for diagnosing peripheral pulmonary lesions since the 1970s.[4,5,7] However, obtaining diagnostic samples from small peripheral pulmonary lesions < 2.0 cm in diameter is difficult.[1–9] In our institute, the diagnostic sensitivity of FFB for small peripheral pulmonary lesions (average diameter, < 20 mm) under radiographic fluoroscopic guidance in the past year was 35%, and the rate for obtaining diagnostic biopsy samples was as low as 13% (data not shown). In the present study, we combined CT-guided TBB, an ultrathin bronchoscope, and VB navigation for diagnosing small peripheral pulmonary lesions. The diagnostic sensitivity of this procedure was as high as 65.4% in small peripheral pulmonary lesions examined in our institute during this period. Moreover, cytologic procedures using brushes or washing might enhance diagnostic sensitivity at least for malignant diseases, although these procedures were not performed in the present study. Notably, all diagnoses were made from biopsy samples, and included two lesions from benign diseases, which have typically been diagnosed from histologic, rather than cytologic, samples. An accurate diagnosis by TBB may circumvent unnecessary surgery with general anesthesia for the treatment of these benign diseases. In addition, even video-assisted thoracoscopic biopsy would retain considerable risk for elderly patients or patients with poor respiratory or cardiac function. For such patients, SRT has been recommended as an appropriate alternative.[23,24] Of the 13 patients found by this procedure to have lung cancer, 5 received SRT and have shown no signs of recurrence for > 1 year. Those cancers may go into complete remission without surgical treatment after accurate diagnosis by bronchoscopy.

We successfully obtained VB images from helical CT scan information, and used them for the simulation and navigation of appropriate bronchial routes to small peripheral pulmonary lesions. Several groups have reported using VB images for the simulation of major endobronchial abnormalities,[25]

and for the assessment of tracheobronchial stenosis[26] and bronchial malignant disease.[27] To navigate cases of thoracic disease, several investigators[28,29] have used VB images for guidance in transbronchial aspiration biopsies of mediastinal lymph nodes. For peripheral lesions, Moriya and colleagues[21] have reported using VB images as a guide for conventional TBB. Furthermore, Asano and colleagues[22] have reported a case of small peripheral pulmonary lesions diagnosed using ultrathin bronchoscopy under VB imaging for bronchoscopic navigation. In cases of TBB using an ultrathin bronchoscope, the bronchoscopists would have to explore many bronchi to reach the lesions, and patients could not tolerate a lengthy procedure. Although HRCT scanning can demonstrate the optimal bronchial path to the lesions, a three-dimensional understanding of the complicated bronchial bifurcation based on axial images is difficult. In this study, VB images were made by a radiologist, but the upcoming development of new software and strategies making VB imaging more convenient will allow respiratory physicians and bronchologists to make VB images from information obtained by helical CT scanning.

Several improvements also may be made to increase the yield of TBB and would bring this procedure into wide use. First, ultrathin bronchoscopes are slightly limp and somewhat difficult to control in the peripheral lung after being bent and turned. In addition, biopsy channels are narrow (diameter, 1.2 mm) and the forceps is small (diameter, 1.0 mm). In this study, six of the nine undiagnosed lesions could not be diagnosed because insufficient tissue specimens could be obtained by biopsy. Brush cytology or bronchial washing may need to be performed together to increase diagnostic sensitivity. CT-guided TBB in combination with VB navigation was performed in an examination time similar to that for conventional TBB. However, the exact radiation exposure to patients and physicians is unknown. Preliminarily, the dose of radiation exposure was measured during an examination of CT-guided TBB. The main operator and three assistants received < 200 microsievert of radiation exposure, which is 1/1,000 less than the dose causing cataracts. A detailed study of radiation exposure and radiation contours in CT scan rooms has to be performed. Moreover, although the total examination time was < 30 min, patients and physicians occupied the CT scan room for approximately 1 h, so the cost of occupying a CT scan room must be considered in terms of hospital economy.

In summary, CT-guided TBB using an ultrathin bronchoscope after VB navigation was performed safely and was very effective for diagnosing small peripheral pulmonary lesions. CT-guided TBB was combined with an ultrathin bronchoscope and VB navigation into one procedure. To clarify the efficacy of each of the three components and the cost/benefit ratio of diagnosing small peripheral pulmonary lesions, randomized trials must be performed.

References

1 Baaklini WA, Reinoso MA, Gorin AB, et al. Diagnostic yield of fiberoptic bronchoscopy in evaluating solitary pulmonary nodules. Chest 2000; 117:1049–1054
2 Shiner RJ, Rosenman J, Katz I, et al. Bronchoscopic evaluation of peripheral lung tumours. Thorax 1988; 43:887–889
3 Chechani V. Bronchoscopic diagnosis of solitary pulmonary nodules and lung masses in the absence of endobronchial abnormality. Chest 1996; 109:620–625
4 Zavala DC. Diagnostic fiberoptic bronchoscopy: techniques and results of biopsy in 600 patients. Chest 1975; 68:12–19
5 Kvale PA, Frederick LTC, Bode R, et al. Diagnostic accuracy in lung cancer. Chest 1976; 69:752–757
6 Stringfield JT, Markowitz DJ, Bentz RR, et al. The effect of tumor size and location on diagnosis by fiberoptic bronchoscopy. Chest 1977; 72:474–476
7 Cortese DA, McDougall JC. Biopsy and brushing of peripheral lung cancer with fluoroscopic guidance. Chest 1979; 75:141–145
8 Mori K, Yanase N, Kaneko M, et al. Diagnosis of peripheral lung cancer in cases of tumors 2 cm or less in size. Chest 1989; 95:304–308
9 Torrington KG, Kern JD. The utility of fiberoptic bronchoscopy in the evaluation of the solitary pulmonary nodule. Chest 1993; 104:1021–1024
10 Sawabata N, Ohta M, Maeda H. Fine-needle aspiration cytologic technique for lung cancer has a high potential of malignant cell spread through the tract. Chest 2000; 118:936–939
11 Seyfer CAE, Walsh DS, Greaber CGM, et al. Chest wall implantation of lung cancer after thin-needle aspiration biopsy. Ann Thorac Surg 1989; 48:284–286
12 Aberle DR, Gamsu G, Golden JA. Fatal systemic arterial air embolism following lung needle aspiration. Radiology 1987; 165:351–353
13 Wong RS, Ketai L, Temes T, et al. Air embolus complicating transthoracic percutaneous needle biopsy. Ann Thorac Surg 1995; 59:1010–1011
14 Larscheid RC, Thorpe PE, Scott WJ. Percutaneous transthoracic needle aspiration biopsy: a comprehensive review of its current role in the diagnosis and treatment of lung tumors. Chest 1998; 114:704–709
15 Kobayashi T, Shimamura K, Hanai K. Computed tomography-guided bronchoscopy with an ultrathin fiberscope. Diagn Ther Endosc 1996; 2:229–232
16 Wagner U, Walthers EW, Gelmetti W, et al. Computer-tomographically guided fiberbronchoscopic transbronchial biopsy of small pulmonary lesions: a feasibility study. Respiration 1996; 63:181–186
17 Kikawada M, Ichinose Y, Miyamoto D, et al. Peripheral airway findings in chronic obstructive pulmonary disease using an ultrathin bronchoscope. Eur Respir J 2000; 15:105–108
18 Rooney CP, Wolf K, McLennan G. Ultrathin bronchoscopy as an adjunct to standard bronchoscopy in the diagnosis of peripheral lung lesions. Respiration 2002; 69:63–68
19 Saka H, Oki M, Kumazawa A, et al. Diagnosis of pulmonary peripheral lesions using an ultrathin bronchoscope. J Jpn Soc Bronchol 2000; 22:617–619

20 Asano F, Kimura T, Shindou J, et al. Usefulness of CT-guided ultrathin bronchoscopy in the diagnosis of peripheral pulmonary lesions that could not be diagnosed by standard transbronchial biopsy. J Jpn Soc Bronchol 2002; 24:80–85
21 Moriya H, Koyama M, Honjo H, et al. Interactive virtual bronchoscopy as a guide for transbronchial biopsy in two cases. J Jpn Soc Bronchol 1998; 20:610–613
22 Asano F, Matsuno Y, Matsushita T, et al. Transbronchial diagnosis of a small peripheral pulmonary lesion using an ultrathin bronchoscope with virtual bronchoscopic navigation. J Bronchol 2002; 9:108–111
23 Fukumoto S, Shirato H, Shimizu S, et al. Small-volume image-guided radiotherapy using hypofractionated, coplanar, and non-coplanar multiple fields for patients with inoperable stage I nonsmall cell lung carcinomas. Cancer 2002; 95:1546–1553
24 Harada T, Shirato H, Ogura S, et al. Real-time tumor-tracking radiation therapy for lung carcinoma by the aid of insertion of a gold marker using bronchofiberscopy. Cancer 2002; 95:1720–1727
25 Vining DJ, Liu K, Choplin RH, et al. Virtual bronchoscopy. Chest 1996; 109:549–553
26 Hoppe H, Walder B, Sonnenschein M, et al. Multidetector CT virtual bronchoscopy to grade tracheobronchial stenosis. Am J Radiol 2002; 178:1195–1200
27 Finkelstein SE, Summers RM, Nguyen DM, et al. Virtual bronchoscopy for evaluation of malignant tumors of the thorax. J Thorac Cardiovasc Surg 2002; 123:967–972
28 McAdams HP, Goodman PC, Kussin P. Virtual bronchoscopy for directing transbronchial needle aspiration of hilar and mediastinal lymph nodes: a pilot study. Am J Radiol 1998; 170:1361–1364
29 Hopper KD, Lucas TA, Gleeson K, et al. Transbronchial biopsy with virtual CT bronchoscopy and nodal highlighting. Radiology 2001; 221:531–536

Reprinted from
Jpn J Clin Oncol 2004;34(9)540–546
doi:10.1093/jjco/hyh098

Cisplatin, Paclitaxel and Escalating Doses of Doxorubicin (TAP) in Advanced Ovarian Cancer: a Phase I Trial

Takashi Onda[1], Noriyuki Katsumata[2], Ryuichiro Tsunematsu[1], Toshiharu Yasugi[3], Masafumi Mushika[4], Kaichiro Yamamoto[5], Tsuneo Fujii[6], Toshio Hirakawa[7], Toshiharu Kamura[8], Toshiaki Saito[9] and Hiroyuki Yoshikawa[10]

[1]Division of Gynecological Oncology and [2]Department of Medical Oncology, National Cancer Center Hospital, Tokyo, [3]Department of Obstetrics and Gynecology, Faculty of Medicine, University of Tokyo, Tokyo, [4]Department of Obstetrics and Gynecology, National Nagoya Hospital, Nagoya, [5]Department of Obstetrics and Gynecology, Sakai Hospital, Kinki University School of Medicine, Sakai, [6]Department of Obstetrics and Gynecology, National Kure Medical Center, Kure, Hiroshima, [7]Department of Obstetrics and Gynecology, Faculty of Medicine, Kyushu University, Fukuoka, [8]Department of Obstetrics and Gynecology, Kurume University School of Medicine, Kurume, Fukuoka, [9]Gynecology Service, National Kyushu Cancer Center, Fukuoka and [10]Department of Obstetrics and Gynecology, Institute of Clinical Medicine, University of Tsukuba, Tsukuba, Ibaraki, Japan

Jpn J Clin Oncol 2004;34(9)540–546
doi:10.1093/jjco/hyh098

Cisplatin, Paclitaxel and Escalating Doses of Doxorubicin (TAP) in Advanced Ovarian Cancer: a Phase I Trial

Takashi Onda[1], Noriyuki Katsumata[2], Ryuichiro Tsunematsu[1], Toshiharu Yasugi[3], Masafumi Mushika[4], Kaichiro Yamamoto[5], Tsuneo Fujii[6], Toshio Hirakawa[7], Toshiharu Kamura[8], Toshiaki Saito[9] and Hiroyuki Yoshikawa[10]

[1]Division of Gynecological Oncology and [2]Department of Medical Oncology, National Cancer Center Hospital, Tokyo, [3]Department of Obstetrics and Gynecology, Faculty of Medicine, University of Tokyo, Tokyo, [4]Department of Obstetrics and Gynecology, National Nagoya Hospital, Nagoya, [5]Department of Obstetrics and Gynecology, Sakai Hospital, Kinki University School of Medicine, Sakai, [6]Department of Obstetrics and Gynecology, National Kure Medical Center, Kure, Hiroshima, [7]Department of Obstetrics and Gynecology, Faculty of Medicine, Kyushu University, Fukuoka, [8]Department of Obstetrics and Gynecology, Kurume University School of Medicine, Kurume, Fukuoka, [9]Gynecology Service, National Kyushu Cancer Center, Fukuoka and [10]Department of Obstetrics and Gynecology, Institute of Clinical Medicine, University of Tsukuba, Tsukuba, Ibaraki, Japan

Received April 3, 2004; accepted June 10, 2004

Background: The objectives of this phase I trial were to determine the maximum tolerated dose (MTD) and the recommended dose (RD) for phase II/III trials of doxorubicin (DOX) combined with paclitaxel (PTX) and cisplatin (CDDP) in patients with advanced ovarian cancer (AOC).
Methods: Twenty-eight patients with stage III/IV AOC received fixed doses of PTX (110 mg/m^2 over 24 h on day 1) and CDDP (75 mg/m^2 on day 2) and an escalating dose of DOX (20, 30, 40 or 50 mg/m^2 on day 1) every 3 weeks. The patients received up to six cycles of chemotherapy. At level 1, one of the original dose-limiting toxicities (DLTs), grade (G) 4 neutropenia lasting for 4 days or longer, occurred in four of six patients. The criterion for DLT was amended to 'G4 neutropenia lasting for 8 days or longer accompanied with G4 leukopenia' and four additional patients were evaluated at level 1.
Results: According to the new criteria, DLT was observed only in one of nine patients except one ineligible patient at level 1and two of six patients at level 4. G4 neutropenia and G4 leukopenia occurred in 85% and 44%, respectively, in the first course of chemotherapy. Non-hematological toxicity was generally mild or moderate. MTD was not determined at the planned dose levels. A clinical response was observed in 16 of 19 (84%) evaluable patients. Further dose escalation was not performed and RD was determined as level 4 because more than 30% of cycles required some modification of chemotherapy at level 4.
Conclusion: The combination of TAP including 50 mg/m^2 of DOX is feasible and well tolerated as first line chemotherapy in AOC, warranting further study of this regimen.

Key words: ovarian cancer – chemotherapy – doxorubicin – phase I study

INTRODUCTION

Since randomized trials have demonstrated the superiority of paclitaxel (PTX) plus cisplatin (CDDP) over cisplatin plus cyclophosphamide (CPA) in overall survival and progression-free survival (1,2) and subsequent trials demonstrated similar activity of PTX plus carboplatin (CBDCA) compared with PTX plus CDDP (3), the combination regimen of PTX plus platinum, such as CDDP or CBDCA, is considered the standard regimen for advanced ovarian cancer (AOC). The two-drug combination regimen of PTX and platinum yields a high response rate and improved survival for patients with AOC. In spite of chemotherapy development, the 5-year survival of patients with stage III/IV ovarian cancer is generally less than or around 20% (4), which is far from satisfactory. Therefore, several approaches, especially new agents or new drug combinations, are being examined in clinical studies to improve further the outcome of treatment for AOC.

Doxorubicin (DOX), an anthracycline, is known to be an active agent for ovarian cancer and was used in combination with CDDP and CPA as a standard regimen for ovarian cancer before the introduction of PTX plus platinum. The benefit of

For reprints and all correspondence: Takashi Onda, Division of Gynecological Oncology, National Cancer Center Hospital, 5-1-1 Tsukiji, Chuo-ku, Tokyo 104-0045, Japan. E-mail: taonda@ncc.go.jp

adding DOX to CDDP and CPA was controversial. A phase III randomized trial of CDDP plus CPA with or without DOX conducted by the Gynecological Oncology Group (GOG) (5) showed no clear benefit of DOX in the pathological complete response rate and median survival time. However, three meta-analyses demonstrated that the incorporation of DOX into the CDDP-based regimen for ovarian cancer may improve the long-term survival of AOC by 7–10% (6–8). Therefore, the value of DOX in the treatment of ovarian cancer was re-examined.

The benefit of adding DOX to the current standard regimen, PTX and platinum, should be evaluated to improve further the outcome of patients with AOC. To evaluate the safety and efficacy of this combination regimen, we conducted a phase I trial in patients with AOC for first-line chemotherapy using a combination of fixed doses of CDDP and PTX with escalating doses of DOX given every 3 weeks.

PATIENTS AND METHODS

SELECTION OF PATIENTS

The subjects of this study were untreated patients with stage IIIC or IV epithelial ovarian cancer. The histology of tumors included serous, mucinous, endometrioid, clear cell, mixed epithelial, undifferentiated, malignant Brenner, transitional cell and unclassified types. Patients with low potential malignancies were not included.

Other eligible criteria for entry into this study were as follows: (a) Eastern Cooperative Oncology Group (ECOG) performance status of 0–2; (b) age 16–75 years; (c) adequate bone marrow function [white blood cell count (WBC) $\geq$3000/mm^3 or absolute neutrophil count (ANC) $\geq$1500/mm^3 and platelet count $\geq$100 000/mm^3], adequate hepatic function [total serum bilirubin $\leq$1.5 mg/dl and serum aspartate aminotransferase (AST) $\leq$2.5 times the upper limit of normal], adequate renal function (serum creatinine $\leq$1.5 mg/dl and creatinine clearance $\geq$50 ml/min) and adequate cardiac function (normal or minor deviation in electrocardiogram); and (d) written informed consent. Patients were ineligible if they had (a) severe mental disorders; (b) uncontrolled hypertension; (c) history of cardiac failure, unstable angina, myocardial infarction within 6 months prior to the study; (d) liver cirrhosis; (e) diabetes mellitus, controlled with insulin; (f) history of severe hypersensitivity or hypersensitivity to drugs formulated with polyoxyethylated castor oil (Cremophor EL) as an ingredient (e.g. cyclosporine or vitamin K); (g) hepatitis B e antigen (HBeAg) or antibody against hepatitis C virus (HCV); or (h) if they were pregnant.

TREATMENT PLAN

All patients underwent staging laparotomy and, simultaneously, maximum cytoreductive surgery. Following surgery, eligible patients were enrolled into the study. Patients received up to six cycles of chemotherapy consisting of paclitaxel (PTX), doxorubicin (DOX) and cisplatin (CDDP). DOX was administered as a 30 min intravenous (IV) infusion on day 1. PTX was administered as a 24 h continuous i.v. infusion on day 1 following DOX administration. CDDP was administered as a 2 h i.v. infusion on day 2. Chemotherapy was repeated every 21 days, assuming recovery from the toxicity of the previous cycle. Four different dose levels were tested. The dose of DOX was escalated from 20 mg/m^2 (level 1) to 50 mg/m^2 (level 4) in increments of 10 mg/m^2 in sequential cohorts and doses of PTX and CDDP were fixed at 110 and 75 mg/m^2, respectively.

A pre-medication schedule consisted of a 20 mg intravenous dexamethasone infusion 12 and 6 h before chemotherapy, 50 mg oral diphenhydramine and 50 mg intravenous ranitidine administration 30 min before chemotherapy. No primary granulocyte colony-stimulating factor (G-CSF) prophylaxis was allowed. G-CSF use was allowed only when grade 4 leukopenia (<1000/m^3) or grade 4 neutropenia (<500/m^3) lasting for 3 days or longer or grade 2 fever ($\geq$38°C) during grade 3 leukopenia (<2000/m^3) or grade 3 neutropenia (<1000/m^3) was observed.

TREATMENT MODIFICATION

Re-treatment was delayed until the following criteria were met. (a) WBC $\geq$2500/mm^3 and platelet count $\geq$100 000/mm^3; (b) total serum bilirubin $\leq$1.5 mg/dl, serum AST $\leq$2.5 times the upper limit of normal and serum creatinine $\leq$1.5 mg/dl; (c) more than 48 h passed after the final G-CSF use; and (d) absence of active infection. Patients were taken out of the study if the treatment interval exceeded 42 days.

For patients experiencing any of the following toxicities, the doses of all three drugs were reduced to 90% of the previous dose: (a) grade 4 leukopenia (<1000/m^3); (b) grade 2 fever ($\geq$38°C) lasting for 3 days and/or bacteremia during grade 3 leukopenia (<2000/m^3) or neutropenia (<1000/m^3); (c) grade 3 thrombocytopenia (<50 000/m^3); and (d) grade 3 or 4 non-hematological toxicities other than nausea and vomiting. Toxicities were graded according to the Japan Clinical Oncology Group (JCOG) toxicity criteria (9), based on Common Toxicity Criteria of the National Cancer Institute (NCI-CTC, 1982) to extend and supplement the criteria.

Chemotherapy was discontinued if (a) response was revealed to be no change (NC) after three cycles of chemotherapy, (b) progressive disease (PD) was observed, (c) unacceptable toxicities were observed or (d) recovery from toxicities was prolonged.

DETERMINATION OF MAXIMUM TOLERATED DOSE AND RECOMMENDED DOSE

The primary objectives of the study were to determine the maximum tolerated dose (MTD) and the recommended dose (RD) of DOX when combined with 110 mg/m^2 of PTX and 75 mg/m^2 of CDDP. Initially, six patients were sequentially enrolled into the lowest dose level. Dose-limiting toxicity

(DLT) was evaluated in the first course of chemotherapy to determine MTD and in all courses of chemotherapy to determine the RD. If none or one of the six patients experienced DLT, then the following six patients would be enrolled into the next dose level. If four or more of the six patients experienced DLT and the dose level was higher than level 1, MTD was determined as the previous dose level. If two or three of the six patients experienced DLT, then an additional six patients would be enrolled into the same dose level at other than level 4. If three or fewer of 12 patients experienced DLT, then the next six patients would be enrolled into the next dose level. If four or more of 12 patients experienced DLT, then MTD was determined as that dose level. These steps were repeated until MTD was determined. RD was determined taking into account the DLT observed in the following courses of chemotherapy.

DLT was initially defined as (a) grade 4 leukopenia ($<1000/m^3$) or grade 4 neutropenia ($<500/m^3$) lasting for 4 days or longer; (b) grade 2 fever ($\geq 38°C$) lasting for 3 days and/or bacteremia during grade 3 leukopenia ($<2000/m^3$) or neutropenia ($<1000/m^3$); (c) grade 4 thrombocytopenia ($<25\,000/m^3$); and (d) grade 3 or 4 non-hematological toxicities other than nausea and vomiting. The criteria were subsequently amended as described in the next subsection.

Amendment of Criteria for Dose-Limiting Toxicity

Among six patients enrolled into dose level 1, grade 4 neutropenia lasting for 4 days or longer [criterion (a)] was observed in four patients during the first course of chemotherapy and neutrophils were not counted in one patient with grade 2 leukopenia. Therefore, the study was discontinued and the toxicities were evaluated. Grade 4 neutropenia was observed for 6–7 days in three patients and observed for 11 days in one patient, although grade 4 leukopenia was not observed. However, all six patients recovered from the toxicity and could receive the subsequent course of chemotherapy without delay. No other DLT was observed in these six patients during the first and subsequent courses. Therefore, dose level 1 was evaluated to be safe and criterion (a) was considered to be too strict. Moreover, many phase I studies for ovarian cancer adopted a criterion of 'grade 4 neutropenia lasting for 8 days or longer' (10–14). Taken together, the following amendment of criteria and study design was permitted by the Data and Safety Monitoring Committee. (1) Criterion (a) was modified to 'grade 4 neutropenia lasting for 8 days or longer accompanied by grade 4 leukopenia for at least 1 day during the period'. According to this amendment, none of the above-mentioned four patients met the criterion. (2) A patient whose neutrophils were not counted was determined to be ineligible. (3) An additional four patients would be enrolled to dose level 1 to determine the safety of the dose level. If DLT was observed in none or one of nine patients, the subsequent patients would be enrolled at dose level 2. If DLT was observed in two of nine patients, an additional three patients would be enrolled at dose level 1. If DLT was observed in three or four of nine patients, the study would be discontinued.

Response Evaluation

A secondary objective of the study was to evaluate the efficacy of the TAP regimen. The World Health Organization (WHO) criteria (15) were employed in this study. Complete response (CR) was defined as the disappearance of all gross evidence of disease for at least 4 weeks. Partial response (PR) was defined as a $\geq 50\%$ reduction in the sum of the products of the two largest perpendicular dimensions of all two-dimensionally measurable lesions and no evidence of new lesions for at least 4 weeks. No change (NC) was defined as a $<25\%$ increase or a $<50\%$ reduction in the sum of the aforementioned products and no evidence of new lesions for at least 4 weeks. Progressive disease (PD) was defined as a $\geq 25\%$ increase in the sum of the above-mentioned products or the appearance of any new lesions. Not evaluable (NE) was defined when insufficient data for response evaluation are available.

Before enrolling the patients into the study, the original protocol was approved by the Institutional Review Board (IRB) in each participating institute. The new protocol including the above-mentioned amendment was also approved by IRB in all participating institutes before restarting the study.

RESULTS

Patients' Characteristics

Between December 1998 and December 2000, 28 patients with advanced ovarian cancer were enrolled in this study. One patient was excluded from the study because sufficient laboratory data were not available for analysis. The median age of the 27 eligible patients was 56 years (range, 24–71 years) and 27 patients received 3–6 courses of chemotherapy (mean, 5.4 courses). Additional patients' characteristics are summarized in Table 1.

Dose Escalation and Dose-Limiting Toxicity

Excluding one ineligible patient, whose neutrophils were not counted during the first course of chemotherapy, nine patients were enrolled into dose level 1. Among these nine patients, only one developed DLT, grade 4 diarrhea, so the dose escalation was allowed. The following six patients were enrolled into dose level 2. These six patients developed no DLT and further dose escalation was performed. The next six patients enrolled into dose level 3 did not develop DLT and the dose was escalated to level 4. Six subsequent patients were enrolled into dose level 4. Two patients developed DLT; one patient developed febrile neutropenia matching criterion (b) and grade 4 diarrhea and another patient developed prolonged grade 4 neutropenia matching criterion (a). The MTD defined in the protocol had not been reached even at dose level 4. Therefore,

Table 1. Patients' characteristics

Characteristic	No. of patients	%
Registered patients	28	–
Eligible patients	27	–
Stage		
III	24	88.9
IV	3	11.1
Histology		
Serous	23	85.2
Endometrioid	2	7.4
Clear cell	1	3.7
Undifferentiated	1	3.7
Residual disease		
0	4	14.8
0–1 cm	6	22.2
1–2 cm	4	14.8
>2 cm	13	48.1

it was decided to determine RD taking into account the toxicities of all cycles, the necessity of G-CSF support, the actual dose delivery and efficacy.

Hematological Toxicity

The hematological toxicity results are summarized in Table 2. The major toxicities observed were neutropenia and leukopenia. Grade 4 neutropenia was observed frequently even during the first course of chemotherapy [85% (23/27)] and almost all patients developed grade 4 neutropenia during all courses of chemotherapy [96% (26/27)]. The dose level was not correlated with the frequency of neutropenia (100% in level 1 and 83% in level 4 during the first course of chemotherapy). Grade 4 leukopenia was observed in 44% (12/27) of patients during the first course and in 52% (14/27) of patients during all courses of chemotherapy. The toxicity did not seem to increase from the second to sixth courses of chemotherapy. However, the frequency of grade 4 leukopenia was correlated with the dose level during the first course [22% (2/9) in level 1 to 83% (5/6) in level 4] and all courses of chemotherapy [22% (2/9) in level 1 to 83% (5/6) in level 4]. Among these grade 4 hematological toxicities observed during the first course of chemotherapy, toxicity developed by one patient in level 4 matched the dose-limiting toxicity criterion (a). As for other hematological toxicity, grade 3 anemia was rarely observed during the first course of chemotherapy [11% (3/27)]; however, nearly half of patients developed grade 3 anemia during all courses of chemotherapy [44% (12/27)]. Grade 4 thrombocytopenia was never observed during the first course of chemotherapy and only one patient developed grade 4 thrombocytopenia during all courses of chemotherapy [4% (1/27)].

Table 2. Hematological toxicity

Toxicity	No.(%) of grade 3/grade 4 toxicity			
	Level 1 (n = 9)	Level 2 (n = 6)	Level 3 (n = 6)	Level 4 (n = 6)
(A) During first course of chemotherapy				
Leukopenia	6 (67)/2 (22)	4 (67)/2 (33)	1 (17)/3 (50)	1 (17)/5 (83)
Neutropenia	0 (0)/9 (100)	1 (17)/4 (67)	0 (0)/5 (83)	1 (17)/5 (83)
Anemia	1 (11)/NA	0 (0)/NA	1 (17)/NA	1 (17)/NA
Thrombocytopenia	0 (0)/0 (0)	0 (0)/0 (0)	0 (0)/0 (0)	0 (0)/0 (0)
(B) During all courses of chemotherapy				
Leukopenia	6 (67)/2 (22)	3 (50)/3 (50)	1 (17)/4 (67)	1 (17)/5 (83)
Neutropenia	0 (0)/9 (100)	1 (17)/5 (83)	0 (0)/6 (100)	0 (0)/6 (100)
Anemia	2 (22)/NA	2 (33)/NA	6 (100)/NA	2 (33)/NA
Thrombocytopenia	0 (0)/0 (0)	1 (17)/0 (0)	2 (33)/0 (0)	1 (17)/1 (17)

Table 3. Non-hematological toxicity

Toxicity	No.(%) of grade 2/grade 3 toxicity			
	Level 1 (n = 9)	Level 2 (n = 6)	Level 3 (n = 6)	Level 4 (n = 6)
(A) During first course of chemotherapy				
Nausea and vomiting	2 (22)/1 (11)	2 (33)/1 (17)	3 (50)/0 (0)	2 (33)/1 (17)
Diarrhea	1 (11)/1 (11)	2 (33)/0 (0)	0 (0)/0 (0)	1 (17)/1 (17)
Alopecia	0 (0)/NA	0 (0)/NA	1 (17)/NA	2 (33)/NA
Neuropathy-sensory	0 (0)/0 (0)	0 (0)/0 (0)	0 (0)/0 (0)	0 (0)/0 (0)
Hypersensitivity	0 (0)/0 (0)	0 (0)/0 (0)	0 (0)/0 (0)	0 (0)/0 (0)
Renal toxicity	0 (0)/0 (0)	0 (0)/0 (0)	0 (0)/0 (0)	0 (0)/0 (0)
Febrile neutropenia	NA/1 (11)	NA/0 (0)	NA/2 (33)	NA/2 (33)
(B) During all courses of chemotherapy				
Nausea and vomiting	5 (55)/1 (11)	2 (33)/1 (17)	4 (67)/0 (0)	4 (67)/1 (17)
Diarrhea	1 (11)/1 (11)	2 (33)/0 (0)	0 (0)/0 (0)	0 (0)/2 (33)
Alopecia	8 (88)/NA	5 (83)/NA	5 (83)/NA	5 (83)/NA
Neuropathy-sensory	0 (0)/0 (0)	0 (0)/0 (0)	0 (0)/0 (0)	1 (17)/0 (0)
Hypersensitivity	0 (0)/0 (0)	0 (0)/0 (0)	0 (0)/0 (0)	0 (0)/0 (0)
Renal toxicity	0 (0)/0 (0)	0 (0)/0 (0)	0 (0)/0 (0)	0 (0)/0 (0)
Febrile neutropenia	NA/2 (22)	NA/0 (0)	NA/2 (33)	NA/2 (33)

Non-hematological Toxicity

The results of non-hematological toxicity are listed in Table 3. Generally, non-hematological toxicity was mild or moderate. The observed grade 3 toxicities during the first course or all courses of chemotherapy were nausea and vomiting in 11% (3/27) or 11% (3/27), diarrhea in 7% (2/27) or 11% (3/27) and febrile neutropenia in 19% (5/27) or 22% (6/27), respectively. The frequency of above grade 3 toxicities did not increase during the second to sixth courses of chemotherapy and was not correlated with the dose levels. Among these grade 3 toxicities observed during the first course of chemotherapy,

Table 4. Clinical response

Clinical response	Level 1 ($n = 9$)	Level 2 ($n = 6$)	Level 3 ($n = 6$)	Level 4 ($n = 6$)	Total
Complete response	4	1	4	3	12
Partial response	1	2	0	1	4
No change	0	0	0	0	0
Progressive disease	0	0	2	1	3
Not evaluable	4	3	0	1	8
Response rate (%)	100 (5/5)	100 (3/3)	67 (4/6)	80 (4/5)	84 (16/19)

two cases of diarrhea, one in level 1 and one in level 4 and one febrile neutropenia in level 4 matched the dose-limiting toxicity criteria (d) and (b). Other than these toxicities, alopecia was the most frequently observed toxicity: 85% (23/27) of patients developed grade 2 alopecia during all courses of chemotherapy. Grade 2/3 hypersensitivity and any grade renal toxicity (rise of serum creatinine) were not observed during the study. It was noteworthy that grade 2/3 sensory neuropathy was not observed during the first course of chemotherapy and only one patient [4% (1/27)] developed grade 2 sensory neuropathy during all courses of chemotherapy.

Clinical Response

Eight patients had no measurable disease at entry. In the other 19 patients with two-dimensionally measurable disease, the response to chemotherapy was evaluated (Table 4). Twelve patients achieved complete response and four achieved partial response. The overall response rate was 84% (16/19) among patients with measurable disease. The remaining three patients had progressive disease. The response rate at dose levels 1–4 was 100, 100, 67 and 80%, respectively, suggesting no correlation between the dose level and response rate.

Recommended Dose

Table 5 summarizes the characteristics of chemotherapy at each level. In level 4, the majority of cycles [91% (30/33)] required G-CSF support and more than 30% of chemotherapy cycles required some modification in the dose or starting date of chemotherapy. However, chemotherapy could be continued until the planned cycle was completed or disease progression in most cases [83% (5/6)]. Moreover, 93.4% of the planned doses of agents could be administered at level 4. Considering all the factors, such as hematological and non-hematological toxicities, clinical responses and actual dose deliveries at dose level 4, RD for further study was decided as dose level 4 consisting of 110 mg/m^2 of PTX, 50 mg/m^2 of DOX and 75 mg/m^2 of CDDP.

DISCUSSION

In this study, we evaluated the safety and efficacy of a combination regimen of PTX, DOX and CDDP (TAP) as first-line

Table 5. Summary of chemotherapies

	Level 1	Level 2	Level 3	Level 4
No. of cycles administered	48	36	32	33
Percentage of cycles required				
G-CSF use	60 (29/48)	72 (26/36)	66 (21/32)	91 (30/33)
Dose reduction	13 (5/39)	7 (2/30)	15 (4/26)	33 (9/27)
Treatment delay	21 (8/39)	20 (6/30)	8 (2/26)	30 (8/27)
Percentage of patients who completed chemotherapy*	67 (6/9)	100 (6/6)	100 (6/6)	83 (5/6)
Average drug administration				
PTX(mg/m^2)	106	108	107	103
DOX(mg/m^2)	19	29	39	47
CDDP(mg/m^2)	72	74	73	70
Percentage of actual/planned doses	96.4	98.2	97.2	93.4

*All six cycles of chemotherapy were completed or chemotherapy was discontinued because of disease progression.

chemotherapy for AOC. Because of the bone marrow toxicity of both CBDCA and DOX, CDDP seems to be safer than CBDCA to combine with DOX as a platinum analog. On the other hand, the combination of CDDP and PTX may produce severe and irreversible neurotoxicity (2,16,17). To avoid this adverse effect and to reduce cardiac toxicity, PTX was administered in a 24 h continuous infusion (18). The PTX dose was set at 110 mg/m^2 as the minimum dose at which sufficient response could be expected, because there is no dose–response relationship in a range of 110 mg/m^2 or more (19). The dose of CDDP was decided as the standard dose of 75 mg/m^2 (20). The DOX dose was increased from 20 to 50 mg/m^2 and was expected to improve efficacy over the standard combination of PTX and platinum. To avoid excessive toxicity, PTX was administered following DOX (21,22) and CDDP was administered following PTX (23). The regimen therefore consisted of 20–50 mg/m^2 increasing doses of DOX followed by 24 h infusion of 110 mg/m^2 of PTX followed by 75 mg/m^2 of CDDP.

Concerning the safety of the regimen, the three-drug combination regimen seemed to be sufficiently safe to use as first-line chemotherapy for patients with ovarian cancer. The major toxicities observed in our study were neutropenia and leukopenia. Grade 4 neutropenia and leukopenia were observed in 85% (23/27) and 44% (12/27) in the first course of chemotherapy. However, these toxicities rarely lasted long enough to be counted as DLT and were not cumulative in the 2nd to 6th courses of chemotherapy. Thus, these hematological toxicities seemed manageable. Moreover, non-hematological toxicities were generally mild or moderate. The grade 3 toxicities observed were nausea and vomiting in 11% (3/27), diarrhea in 11% (3/27) and febrile neutropenia in 22% (6/27), during all courses

of chemotherapy. Grade 3 sensory neuropathy was not observed during all courses of chemotherapy. To our knowledge, seven phase I or I/II studies (10,24–29), evaluating the value of anthracyclines in a taxane and platinum-based regimen for previously untreated AOC, have been published. The major toxicities observed throughout the studies were hematological toxicities, such as neutropenia, leukopenia and thrombocytopenia. In particular, neutropenia was reported in 100% in some studies (25,27,28). However, the toxicity was readily managed using G-CSF and was rarely complicated with serious infection or sepsis. Non-hematological toxicities, excluding nausea, vomiting and alopecia, were generally mild and manageable. No severe cardiac toxicity or neuropathy was observed throughout the previous studies.

As for the efficacy of the triplet combination in our study, a response rate (RR) of 84% (16/19), including 63% (12/19) complete response (CR), was observed. Even in level 1, 100% RR was achieved and there was no correlation between the dose level and response rate. In the previous studies, that using docetaxel (DOC) as the taxane (28) showed a relatively lower response rate of 36%, but studies using PTX as the taxane showed a higher response rate of 83–100%. In studies using PTX, there were no apparent differences in the response rate between studies using CDDP (86–100%) (25,26) and those using CBDCA (83–100%) (10,24,29) as platinum compound and between studies using DOX (100%) (24,25) and those using EpiDOX (83–86%) (10,26,29) as anthracycline.

In summary, the combination regimen of DOX with PTX and CDDP is highly active and hematological toxicities are readily manageable and non-hematological toxicities, including cardiac toxicity and sensory neuropathy, were mild or moderate. From our study and previous studies, we conclude that the addition of anthracyclines to PTX plus a platinum-based regimen may provide an effective and safe regimen for patients with untreated ovarian cancer. However, the hematological toxicities seem to be relatively severe compared with those reported with a PTX/CBDCA combination (3,30,31). At present, AGO–GINECO (Arbeitsgemeinschaft Gynäkologische Onkologie–Groupe d'Investigateurs Nationaux pour l'Etude des Cancers Ovariens) (32) and NSGO–EORTC–NCIC CTG (Nordic Society of Gynecological Oncology–European Organization for Research and Treatment of Cancer–National Cancer Institute of Canada Clinical Trials Group) (33) are conducting phase III studies comparing epirubicin/paclitaxel/carboplatin vs. paclitaxel/carboplatin. To assess the usefulness of anthracyclines, the results of these studies are awaited.

Acknowledgments

We thank Dr Nagahiro Saijo for his support and suggestions as a member of Data and Safety Monitoring Committee of this study.

References

1. McGuire WP, Hoskins WJ, Brady MF, Kucera PR, Partridge EE, Look KY, et al. Cyclophosphamide and cisplatin compared with paclitaxel and cisplatin in patients with stage III and stage IV ovarian cancer. *N Engl J Med* 1996;334:1–6.
2. Piccart MJ, Bertelsen K, James K, Cassidy J, Mangioni C, Simonsen E, et al. Randomized intergroup trial of cisplatin–paclitaxel versus cisplatin–cyclophosphamide in women with advanced epithelial ovarian cancer: three-year results. *J Natl Cancer Inst* 2000;92:699–708.
3. Ozols RF, Bundy BN, Greer BE, Fowler JM, Clarke-Pearson D, Burger RA, et al. Phase III trial of carboplatin and paclitaxel compared with cisplatin and paclitaxel in patients with optimally resected stage III ovarian cancer: a Gynecologic Oncology Group study. *J Clin Oncol* 2003;21:3194–200.
4. Nguyen HN, Averette HE, Hoskins W, Sevin BU, Penalver M, Steren A. National survey of ovarian carcinoma. VI. Critical assessment of current International Federation of Gynecology and Obstetrics staging system. *Cancer* 1993;72:3007–11.
5. Omura GA, Bundy BN, Berek JS, Curry S, Delgado G, Mortel R. Randomized trial of cyclophosphamide plus cisplatin with or without doxorubicin in ovarian carcinoma: a Gynecologic Oncology Group study. *J Clin Oncol* 1989;7:457–65.
6. Cyclophosphamide plus cisplatin versus cyclophosphamide, doxorubicin and cisplatin chemotherapy of ovarian carcinoma: a meta-analysis. The Ovarian Cancer Meta-Analysis Project. *J Clin Oncol* 1991;9:1668–74.
7. Fanning J, Bennett TZ, Hilgers RD. Meta-analysis of cisplatin, doxorubicin and cyclophosphamide versus cisplatin and cyclophosphamide chemotherapy of ovarian carcinoma. *Obstet Gynecol* 1992;80:954–60.
8. A'Hern RP, Gore ME. Impact of doxorubicin on survival in advanced ovarian cancer. *J Clin Oncol* 1995;13:726–32.
9. Tobinai K, Kohno A, Shimada Y, Watanabe T, Tamura T, Takeyama K, et al. Toxicity grading criteria of the Japan Clinical Oncology Group. The Clinical Trial Review Committee of the Japan Clinical Oncology Group. *Jpn J Clin Oncol* 1993;23:250–7.
10. du Bois A, Luck HJ, Bauknecht T, Meier W, Richter B, Kuhn W, et al. First-line chemotherapy with epirubicin, paclitaxel and carboplatin for advanced ovarian cancer: a phase I/II study of the Arbeitsgemeinschaft Gynäkologische Onkologie Ovarian Cancer Study Group. *J Clin Oncol* 1999;17:46–51.
11. Siddiqui N, Boddy AV, Thomas HD, Bailey NP, Robson L, Lind MJ, et al. A clinical and pharmacokinetic study of the combination of carboplatin and paclitaxel for epithelial ovarian cancer. *Br J Cancer* 1997;75:287–94.
12. Bolis G, Scarfone G, Villa A, Acerboni S, Siliprandi V, Guarnerio P. A phase I trial with fixed-dose carboplatin and escalating doses of paclitaxel in advanced ovarian cancer. *Semin Oncol* 1997;24, No 1, Suppl 2:23–5.
13. Huizing MT, van Warmerdam LJ, Rosing H, Schaefers MC, Lai A, Helmerhorst TJ, et al. Phase I and pharmacologic study of the combination paclitaxel and carboplatin as first-line chemotherapy in stage III and IV ovarian cancer. *J Clin Oncol* 1997;15:1953–64.
14. ten Bokkel Huinink WW, Veenhof C, Huizing M, Rodenhuis S, Helmerhorst T, Dubbelman R, et al. Carboplatin and paclitaxel in patients with advanced ovarian cancer: a dose-finding study. *Semin Oncol* 1997;24, No 1, Suppl 2:31–3.
15. Miller AB, Hoogstraten B, Staquet M, Winkler A. Reporting results of cancer treatment. *Cancer* 1981;47:207–14.
16. Rowinsky EK, Chaudhry V, Forastiere AA, Sartorius SE, Ettinger DS, Grochow LB, et al. Phase I and pharmacologic study of paclitaxel and cisplatin with granulocyte colony-stimulating factor: neuromuscular toxicity is dose-limiting. *J Clin Oncol* 1993;11:2010–20.
17. Chaudhry V, Rowinsky EK, Sartorius SE, Donehower RC, Cornblath DR. Peripheral neuropathy from taxol and cisplatin combination chemotherapy: clinical and electrophysiological studies. *Ann Neurol* 1994;35:304–11.
18. Smith RE, Brown AM, Mamounas EP, Anderson SJ, Lembersky BC, Atkins JH, et al. Randomized trial of 3-hour versus 24-hour infusion of high-dose paclitaxel in patients with metastatic or locally advanced breast cancer: National Surgical Adjuvant Breast and Bowel Project Protocol B-26. *J Clin Oncol* 1999;17:3403–11.
19. Rowinsky EK, Mackey MK, Goodman SN. Meta analysis of paclitaxel dose–response and dose–intensity in recurrent or refractory ovarian cancer. *Proc Am Soc Clin Oncol* 1996;15:Meeting Abstract.

20. Kaye SB, Paul J, Cassidy J, Lewis CR, Duncan ID, Gordon HK, et al. Mature results of a randomized trial of two doses of cisplatin for the treatment of ovarian cancer. Scottish Gynecology Cancer Trials Group. *J Clin Oncol* 1996;14:2113–9.
21. Sledge GW Jr, Robert N, Sparano JA, Cobeligh M, Goldstein LJ, Neuberg D, et al. Paclitaxel (taxol)/doxorubicin combinations in advanced breast cancer: the Eastern Cooperative Oncology Group experience. *Semin Oncol* 1994;21:15–8.
22. Sledge GW Jr, Robert N, Sparano JA, Cogleigh M, Goldstein LJ, Neuberg D, et al. Eastern Cooperative Oncology Group studies of paclitaxel and doxorubicin in advanced breast cancer. *Semin Oncol* 1995;22:105–8.
23. Rowinsky EK, Gilbert MR, McGuire WP, Noe DA, Grochow LB, Forastiere AA, et al. Sequences of taxol and cisplatin: a phase I and pharmacologic study. *J Clin Oncol* 1991;9:1692–703.
24. Hill M, Macfarlane V, Moore J, Gore ME. Taxane/platinum/anthracycline combination therapy in advanced epithelial ovarian cancer. *Semin Oncol* 1997;24, No 1, Suppl 2:34–7.
25. Naumann RW, Alvarez RD, Omura GA, Segars E, Kilgore LC, Partridge EE. A phase I study of paclitaxel, doxorubicin and cisplatin in patients with previously untreated epithelial ovarian cancer. *Gynecol Oncol* 1998;71:450–3.
26. Papadimitriou CA, Moulopoulos LA, Vlahos G, Voulgaris Z, Kiosses E, Georgoulias N, et al. Paclitaxel, cisplatin and epirubicin first-line chemotherapy in stage III and IV ovarian carcinoma: long-term results of a phase II study. *Cancer* 2000;89:1547–54.
27. Gregory RK, Hill ME, Moore J, A'Hern RP, Johnston SR, Blake P, et al. Combining platinum, paclitaxel and anthracycline in patients with advanced gynaecological malignancy. *Eur J Cancer* 2000;36:503–7.
28. O'Neill VJ, Kaye SB, Reed NS, Paul J, Davis JA, Vasey PA. A dose-finding study of carboplatin–epirubicin–docetaxel in advanced epithelial ovarian cancer. *Br J Cancer* 2002;86:1385–90.
29. Romanini A, Tanganelli L, Carnino F, Fanucchi A, Lionetto R, Pastorino S, et al. First-line chemotherapy with epidoxorubicin, paclitaxel and carboplatin for the treatment of advanced epithelial ovarian cancer patients. *Gynecol Oncol* 2003;89:354–9.
30. Neijt JP, Engelholm SA, Witteveen PO, Tuxen MK, Sorensen PG, Hansen M, et al. Paclitaxel (175 mg/m^2 over 3 h) with cisplatin or carboplatin in previously untreated ovarian cancer: an interim analysis. *Semin Oncol* 1997;24, No 5, Suppl 15:36–9.
31. du Bois A, Luck HJ, Meier W, Mobus V, Costa S, Richter B, et al. Carboplatin/paclitaxel versus cisplatin/paclitaxel as first-line chemotherapy in advanced ovarian cancer: an interim analysis of a randomized phase III trial of the Arbeitsgemeinschaft Gynakologische Onkologie Ovarian Cancer Study Group. *Semin Oncol* 1997;24, No 5, Suppl 15: 44–52.
32. du Bois A, Weber B, Pfisterer J, Goupil A, Wagner U, Barats J, et al. Epirubicin/paclitaxel/carboplatin (TEC) vs. paclitaxel/carboplatin (TC) in first-line treatment of ovarian cancer FIGO stages IIb/IV. Interim results of an AGO/GINECO Intergroup Phase III trial. *Proc Am Soc Clin Oncol* 2001;20:Abstract 805.
33. Kristensen G, Vergote I, Stuart G, Izqiuerdo Delso M, Mirza MR, Aavall-Lundquist E, et al. First line treatment of ovarian cancer FIGO stages IIb–IV with paclitaxel/epirubicin/carboplatin (TEC) vs. paclitaxel/carboplatin (TC). Interim results of an NSGO–EORTC–NCIC CTG Gynecological Cancer Intergroup phase III trial. *Proc Am Soc Clin Oncol* 2002;21:Abstract 805.

American Journal of Pathology, Vol. 164, No. 2, February 2004

Increased DNA Methyltransferase 1 (DNMT1) Protein Expression Correlates Significantly with Poorer Tumor Differentiation and Frequent DNA Hypermethylation of Multiple CpG Islands in Gastric Cancers

Tsuyoshi Etoh,*† Yae Kanai,* Saori Ushijima,* Tohru Nakagawa,* Yukihiro Nakanishi,* Mitsuru Sasako,‡ Seigo Kitano,† and Setsuo Hirohashi*

From the Pathology Division, National Cancer Center Research Institute, Tokyo, Japan; the Gastric Surgery Division,‡ National Cancer Center Hospital, Tokyo, Japan; and the Department of Surgery I,† Oita Medical University, Oita, Japan*

We evaluated the significance of aberrant DNA methyltransferase 1 (DNMT1) protein expression during gastric carcinogenesis. The protein expression of DNMT1, Muc2, human gastric mucin, E-cadherin, and proliferating cell nuclear antigen was examined immunohistochemically in gastric cancers and corresponding noncancerous mucosae from 134 patients. The DNA methylation status of the CpG islands of the *p16*, *human MutL homologue 1 (hMLH1)*, *E-cadherin*, and *thrombospondin-1 (THBS-1)* genes and the methylated in tumor (MINT)-1, -2, -12, and -31 clones was examined by methylation-specific polymerase chain reaction and combined bisulfite restriction enzyme analysis. Epstein-Barr virus (EBV) infection was detected by *in situ* hybridization. Nuclear immunoreactivity for DNMT1 was not detected in any of the noncancerous epithelia, except in proliferative zones (positive internal control), but was found in 97 (72%) of the gastric cancers. DNMT1 overexpression correlated significantly with poorer tumor differentiation ($P < 0.001$), but not with the phenotype (gastric type *versus* intestinal type) of the cancer cells. It also correlated significantly with DNA hypermethylation of the CpG islands of the *hMLH1* ($P = 0.024$) and *THBS-1* genes ($P = 0.043$), and with the CpG island methylator phenotype in the gastric cancers ($P = 0.007$). Reduced E-cadherin expression correlated significantly with poorer tumor differentiation ($P = 0.002$), DNA hypermethylation of the *E-cadherin* gene ($P < 0.001$) and DNMT1 overexpression ($P = 0.014$). DNMT1 overexpression was also associated with EBV infection (a potential etiological factor in gastric carcinogenesis) but not with the proliferative activity of the cancer cells as indicated by the proliferating cell nuclear antigen-labeling index. These results suggest that DNMT1 overexpression may not be just a secondary effect of increased cancer cell proliferative activity, but may be associated with EBV infection and other etiological factors during gastric carcinogenesis. Furthermore, DNMT1 may play a significant role in the development of poorly differentiated gastric cancers by inducing frequent DNA hypermethylation of multiple CpG islands. *(Am J Pathol 2004, 164:689–699)*

DNA methylation plays an important role in transcriptional regulation and chromatin remodeling in mammalian cells.[1] Both overall DNA hypomethylation and more regional DNA hypermethylation have been well documented in various cancers.[1–8] Aberrant DNA methylation may be involved in carcinogenesis as a result of 1) increased gene mutagenicity because of deamination of 5-methylcytosine to thymine; 2) a possible association of aberrant DNA methylation with allelic loss; and 3) repression of gene transcription through methylation of CpG islands in regulatory regions of specific genes, including tumor-suppressor genes.[1]

To date, three enzymes, DNA methyltransferase 1 (DNMT1),[9] DNMT3a, and DNMT3b,[10] have been confirmed to possess DNMT activity. Of these, DNMT1 is the major and best known. As DNMT1 shows a preference for hemimethylated rather than unmethylated substrates *in vitro*,[11] and targets replication foci by binding to proliferating cell nuclear antigen (PCNA),[12] it seems to be a

Supported by a Grant-in-Aid for the Second Term Comprehensive 10-Year Strategy for Cancer Control; a Grant-in-Aid for Cancer Research from the Ministry of Health, Labor, and Welfare of Japan; and a research resident fellowship from the Foundation for Promotion of Cancer Research in Japan (to T.N.).

Accepted for publication October 8, 2003.

Address reprint requests to Yae Kanai, Pathology Division, National Cancer Center Research Institute, 5-1-1 Tsukiji, Chuo-ku, Tokyo 104-0045, Japan. E-mail: ykanai@ncc.go.jp.